

# Fracture Mechanics Model of Anchor Group Breakout

R. Ballarini, F. ASCE<sup>1</sup>; and X. Yueyue<sup>2</sup>

**Abstract:** Linear elastic fracture mechanics-based discrete crack propagation simulations are presented as the pullout of an anchor group from a concrete matrix. The group was modeled as a periodic arrangement of anchors and load-carrying capacities and crack paths were determined as functions of relative depth and spacing. The results suggest that American Concrete Institute design formulas for predicting the capacity of group anchors are highly conservative, and that three-dimensional fracture mechanics-based simulations offer great promise for improving design formulas associated with specific anchor geometries and loadings. DOI: 10.1061/(ASCE)EM.1943-7889.0001200. © 2016 American Society of Civil Engineers.

**Author keywords:** Concrete anchor group; Breakout simulations; Anchorage.

## Introduction

Predicting the tensile load-carrying capacity of a steel anchor embedded at depth  $d$  within a concrete matrix, for the case in which the concrete progressively fractures and breaks out as a cone, remained a relatively difficult and not well-understood problem up to the early 1980s (Klinger and Mendonca 1982). This is because fracture mechanics of concrete structures was still in its early stages, and it had not been discovered that the breakout process is in the realm of fracture mechanics. In fact, up to that time, the debate was centered around which strength property of concrete plays the critical role in resisting failure, what deformation mechanisms are involved in the progressive breakout process, and whether additional understanding could be derived using improved plasticity and damage-based procedures. Within the context of strength-based theories, some investigators argued that the load-carrying capacity depended on the concrete compressive strength, whereas others proposed dependencies on shear strength or tensile strength. Therefore, design codes continued to rely on formulas derived from relatively simple limit-state models that assumed the maximum load was in equilibrium with the resultant of uniformly distributed stresses acting on the surface of a pullout cone with prescribed shape. Regardless of the differences between numerous plasticity-based models that were proposed to improve on predictions, their reliance on a limiting stress automatically conferred on their load-carrying capacity the  $d^2$ -dependence that prevailed in design formulas as recently as 1989 [ACI Committee 349 (ACI 1989)]. Fig. 1 shows that the plasticity-based design formulas represent the limit state calculation involving the assumption of a failure cone that resists the pullout force through a traction distribution proportional to the tensile strength of the concrete,  $f_t$ . The geometric parameters in this figure are those that appear in the ACI code, namely the effective embedment depth  $h_{ef}$  and the anchor diameter  $d_u$ . For convenience and to reduce the number of subscripts in the

equations of this paper, these parameters are redefined as follows:  $h_{ef} \equiv d$ , and  $d_u \equiv c$ . The load-carrying capacity was determined in the obsolete design procedures developed in the ACI Code by Committee 349-89 (ACI 1989) by the limit-load formula

$$P_{u,ACI} = f_t \pi d^2 \left(1 + \frac{c}{d}\right) = 4\phi \sqrt{f'_c} \pi d^2 \left(1 + \frac{c}{d}\right) \approx f_t d^2 \quad (1)$$

In Eq. (1), the tensile strength has been related to the compressive strength,  $f'_c$ , through the strength reduction factor  $\phi$  ( $f_t = 4\phi \sqrt{f'_c}$ ).

Advances in fracture mechanics modeling of concrete structures led to theoretical, computational, and experimental studies, starting in the early 1980s and continuing to today, that relied on the linear elastic fracture mechanics (LEFM) assumption that the load carrying capacity is dictated by the concrete fracture toughness,  $K_c$ , and, in turn, obeys the  $d^{3/2}$  dependence that is consistent with experimental data, linearity, and dimensional analysis (Ballarini et al. 1986, 1987; Elfgren 1998; Elfgren and Ohlson 1992; Eligehausen and Sawade 1989; Eligehausen and Balogh 1995; Eligehausen et al. 2006; Fuchs et al. 1995; Karihaloo 1996; Krenchel and Shah 1985; Ozbolt and Eligehausen 1992; Ozbolt et al. 1999; Vogel and Ballarini 1999; Piccinin et al. 2010, 2012). The load-carrying capacity predicted by LEFM, referred to as concrete capacity design (CCD), can be written as

$$P_{LEFM} \approx K_c d^{3/2} \approx k_c \sqrt{f'_c} d^{3/2} \quad (2)$$

where  $k_c$  = experimentally determined factor introduced by Fuchs et al. (1995) to relate concrete's fracture toughness to its compressive strength. The plasticity-based design formulas in the design codes have been replaced with the LEFM-derived  $d^{3/2}$  dependence as evidenced by the procedures spelled out in Comité Euro-International du Béton (CEB), ACI Committee 349 (ACI 2006), and ACI Committee 318 (ACI 2008). The success of LEFM in the design of steel to concrete anchorage cannot be overstated; it paves the way for future contributions of LEFM to the design of concrete structures as evidenced by current discussions in the concrete community to introduce size effects in the design procedures for shear and torsion loadings.

The fracture behavior of anchors being pulled out of concrete is associated with the strongest possible size effect, which is the negative square root dependence of ultimate stress on structural size dictated by LEFM. The reason for this remarkable result is that

<sup>1</sup>Professor, Dept. of Civil and Environmental Engineering, Univ. of Houston, Houston, TX 77204 (corresponding author). E-mail: rballarini@uh.edu

<sup>2</sup>Engineer, Tolunay-Wong Engineers, Inc., 10710 S. Sam Houston Parkway W, Houston, TX 77031.

Note. This manuscript was submitted on June 7, 2016; approved on September 30, 2016; published online on November 29, 2016. Discussion period open until April 29, 2017; separate discussions must be submitted for individual papers. This paper is part of the *Journal of Engineering Mechanics*, © ASCE, ISSN 0733-9399.

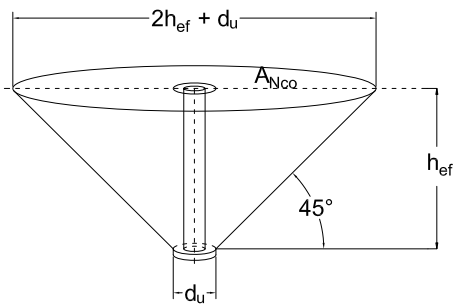


**Fig. 1.** Failure surface assumed by the first ACI Code provision (ACI 1989)

the pullout configuration is, in the parlance of crack analysis, a highly positive geometry. In fact Piccinin et al. (2012) showed that LEM suffices through experiments, and showed that the load-carrying capacities and crack paths predicted by LEM are approximately equal to those predicted by the cohesive zone models that typically are used to account for the size effects exhibited by most concrete structures. Specifically they showed that LEM suffices even if the embedment depth, which represents the most significant characteristic dimension of the structure, is comparable to the aggregate size. It is for this reason that the model presented in this paper relied confidently on LEM.

The role played by the surface of the cone that is produced as the anchor breaks out from the matrix is another extremely important difference between plasticity-based formulas and those derived from fracture mechanics. The previously discussed  $d^2$  scaling results from the assumption that the load-carrying capacity increases in proportion to the cone's surface area. Although fracture mechanics simulations have made it abundantly clear that the relationship does not hold; the crack front that extends from the edge of the anchor toward the free surface becomes unstable under load-control long before it reaches the surface. Thus, the capacity does not scale with the surface area of the cone. The process of crack propagation in the breakout process is analogous to a zipper that has been loaded with a critical weight. Once it starts to unzip, its load-carrying capacity in no way increases in proportion to the length of the portion of the zipper that has not yet unzipped.

Despite this important difference, the area of the pullout cone still enters in the design formulas for group anchors and anchors near free edges, and, in particular, in how it is prescribed at which spacing anchors sense each others' presence. Specifically, anchors are assumed to interact with each other and influence the load-carrying capacity when the surfaces of their respective cones coalesce. If the crack front for closely spaced anchors becomes unstable under force control at lengths that are significantly shorter than the total length traveled to the free surface, then it is expected that the design formulas are overly conservative. Indeed, the ACI (2008) commentary paragraph RD.5.2.3 states: "For anchors located less than  $1.5h_{ef}$  from three or more edges ( $h_{ef}$  is the effective embedment depth), the tensile breakout strength computed by the CCD method, which is the basis for Eq. (D-4)–(D-11), gives overly conservative results. This occurs because the ordinary definitions of  $A_{Nc}/A_{Nco}$  (the ratio of the projected areas of the breakout cone associated with a group of  $N$  anchors and an isolated anchor, respectively) do not correctly reflect the edge effects." The commentary then continues with modifications to the design formulas that reduce the conservatism in the design, with certain restrictions.

This paper is not intended to provide new and improved design formulas, or to compare its results with experimental results

obtained on anchor groups of specific configurations (this clearly cannot be done because of differences in geometry between the idealized model considered in this paper and the more complex configurations encountered in practice). These important tasks are beyond the scope of the paper and will require substantial effort by the concrete community. Instead, this paper focuses on identifying and quantifying one factor that contributes to the overly conservative nature of the design formulas available for designing anchor groups that have been recognized by the ACI commentary quoted previously. Through the analysis of a simplified configuration that is amenable to relatively simple axisymmetric analysis, this paper makes the argument that one of the reasons the design formulas for anchor groups are overly conservative is that they maintain that the load-carrying capacity depends on the projected area of the failure cone. This occurs despite the fact that the lack of dependence of the capacity on the area of the failure surface is, in essence, the reason why fracture mechanics has been successful in the design of individual anchors. Specifically, the simplified model will show that because the ultimate load is achieved when the cracks that initiate at the anchors' edges are relatively short, the reduction of load-carrying capacity with decreasing anchor spacing is smaller than what is predicted by the design formulas.

## LEFM Model and Nondimensional Parameters

Fig. 2(a) shows the anchor group whose failure was investigated using incremental discrete crack propagation simulations enabled by the software (*FRANC-2D*). This simplified periodic hexagonal arrangement represents the limit of  $N = \infty$  equally spaced anchors. The simplified configuration cannot be used directly to quantify the reduction of load-bearing capacity for an anchor group whose perimeter-defining anchors interact with a traction-free boundary. However, this geometry captures the essence of the interaction between the anchors, namely the anchor spacing and embedment depth, and its symmetries allow it to be modeled using the single unit cell shown in Fig. 2(b). Fig. 2(b) also shows that the approximation as a cylinder of the (three-dimensional) hexagonal outer surface of the unit cell reduces the problem to a (two-dimensional) axisymmetric representation. The symmetries and axial constraint at infinity are represented by the zero shear stress condition and zero horizontal displacement along the vertical exterior surfaces of a section of the axisymmetric configuration as shown in Fig. 2(b). The periodicity assumes all anchors break out simultaneously.

The relevant dimensions of the model are the embedment depth,  $d$ , anchor spacing,  $s$ , and anchor diameter,  $c$ . The headed anchor is represented, as was done in Ballarini et al. (1986), Ballarini et al. (1987), Vogel and Ballarini (1999), and Piccinin et al. (2010, 2012) by a discontinuity whose top surface is restrained from displacing in the vertical and horizontal directions, and its lower surface is traction-free. This simplification eliminates the need to model the anchor thickness and for the presence of the steel stem, and has been shown to accurately capture the crack paths and the load-carrying capacity associated with an isolated anchor (Ballarini et al. 1986). The crack length,  $l$ , is defined as the curvilinear distance of the traction-free crack front from the edge of the anchor. The pullout force acting on the anchor,  $P$ , is equal to the resultant of the vertical nodal forces on the top surface of the discontinuity produced by a uniform stress,  $p$ , applied along the bottom surface of the cylindrical model. It is recognized that in anchorage applications, the pullout force not always is transmitted to the lower surface as indicated in Fig. 2(b). However, as demonstrated in the previously cited models that led to the currently used fracture mechanics-based design formulas, the uniform stress is but a way

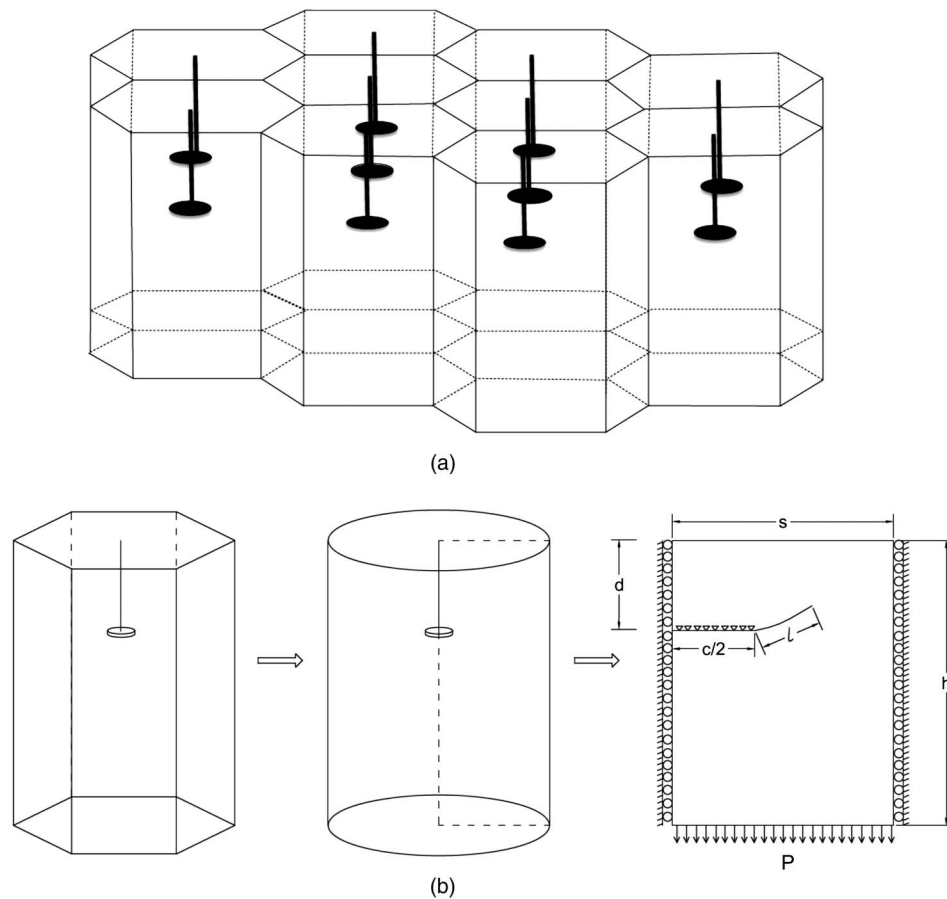


**Fig. 2.** (a) Hexagonal periodic arrangement of anchor group; (b) unit cell; (c) cylindrical approximation of unit cell; (d) axisymmetric section of cylindrical unit cell

of maintaining equilibrium and it does not affect the dependence of the load-carrying capacity on embedment depth. Also not affecting the scaling law, is the compressive stress-induced damage in the concrete in the immediate vicinity of the anchor tops that are embedded relatively deeply. Such damage may have a small effect on the very initial shape of the crack path, but not on the overall shape of the pullout cone and on the fracture-energy dominated load-carrying capacity. The effects of loading type; secondary damage, such as compressive stress-induced microcracking in the vicinity of the anchor; and other types of uncertainties are good reasons why the design codes incorporate a highly conservative approach to the design of embedded anchors. Nevertheless, the simplified model presented in this paper is sufficient to illustrate the irrelevance of the projected area of the failure surface to the load-carrying capacity of an anchor group.

*FRANC-2D* possesses the ability to automatically remesh as it extends the crack according to several choices of crack extension direction criteria that depend on the Mode-I and Mode-II stress intensity factors. The simulations presented in this paper rely on stress intensity factors calculated using the *J*-integral method, which were used to determine the direction of crack extension according to the maximum hoop stress criterion (*FRANC-2D*). According to this local symmetry criterion, the crack chooses a path that renders the Mode-II stress intensity factor nearly zero. Furthermore, the crack length is in equilibrium with the applied force according to the Griffith criterion; its Mode-I stress intensity factor,  $K_I$ , is equal to the concrete fracture toughness,  $K_{Ic}$ .

Following Vogel and Ballarini (1999), linearity and dimensional consistency require that for the applied loading to be in equilibrium with the crack length, according to the Griffith criterion, the fracture toughness could be related to the applied force as

$$K_{Ic} = P_c d^{-3/2} f \left( \frac{l}{c}, \frac{d}{c}, \frac{s}{d}, \nu \right) \quad (3)$$

where  $f$  is determined from the simulations; and  $\nu$  = Poisson's ratio (set equal to 0.2 in all calculations). The normalized maximum force achieved as the crack extends from the edge of the anchor to the free surface is therefore expressed as

$$\frac{P_c}{K_{Ic} d^{3/2}} \equiv g = \min \left( \frac{1}{f} \right) \quad (4)$$

where min = minimum Mode-I stress intensity factor calculated along the crack path.

## Results

A representative finite element method mesh is shown in Fig. 3. The load-carrying capacities and crack paths presented next represent the converged results as obtained by performing simulations with meshes of varying element density for every geometry. The purpose of Fig. 3 is to illustrate that the initial mesh must be tailored to accommodate the automatic mesh refinement that

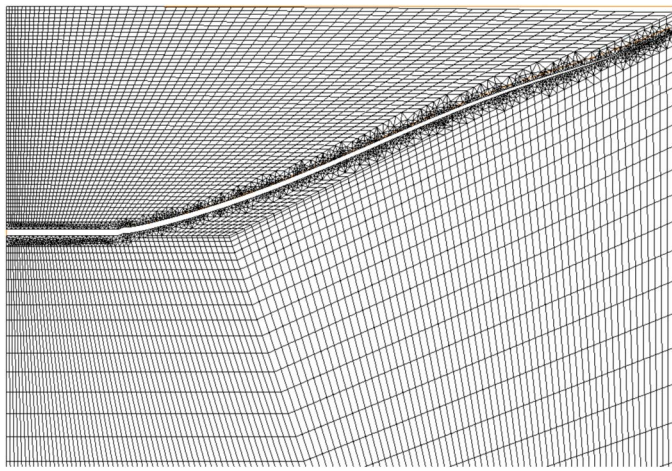


**Fig. 3.** Representative finite element mesh showing the density of elements at the end of a breakout simulation

is performed by *FRANC-2D* after each crack extension increment. The accuracies of the stress intensity factors, load-carrying capacities, and crack paths calculated using *FRANC-2D* for axisymmetric curvilinear crack paths have been reported for crack configurations very similar to the one studied in this paper by Gordeliy et al. (2013). Gordeliy's results were obtained using a displacement discontinuity-based integral equation approach, and, as far as the authors know, it is the only convincing solution procedure in the literature on such problems. Additional confidence in the results comes from a favorable comparison with the isolated anchor results presented in Piccinin et al. (2012); the differences in load capacities were shown to be less than 5%, and the crack paths were indistinguishable. *FRANC-2D* calculates the stress intensity factors using two approaches: the displacement correlation technique and the *J*-integral procedure. The mentioned small differences between the results presented in this paper and those in Piccinin et al. (2012) are because of differences in the method used to evaluate the stress intensity factors; in Piccinin et al. (2012) the displacement correlation technique was used. The method chosen in this paper is the latter because it generally is accepted that it is deemed more

accurate as a result of comparisons with benchmark solutions over the program's life, including comparisons with Gordeliy et al.'s (2013) convincing results.

### Crack Paths

Representative crack paths are shown in Fig. 4 as functions of normalized embedment depth,  $d/c = 1, 2, 5,$  and  $10$ , for selected values of normalized anchor spacing,  $s/d = 5, 3,$  and  $1.5$ . The path for  $d/c = 10$  starts at the left-most point, the  $d/c = 5$  path starts immediately to its right, and so forth. The paths for  $d/c = 10$  and  $d/c = 5$  are hardly distinguishable. These figures also indicate the point at which crack propagation becomes unstable under load control, as discussed subsequently. It was determined that for  $s/d > \sim 3$ , and as shown in the figure, the crack path crossed the free surface at a significantly large horizontal distance from the vertical boundary of the unit cell. Thus, the cone produced by one anchor did not interact with the one produced by its nearest neighbors. The lack of interaction was underscored by the observation that the maximum load was reached at crack lengths that were less than 30% of the total length they traveled before breaking the free surface. When  $s/d \sim 3$ , the crack front broke the surface at the edge of the boundary of the unit cell, thus forming a connection with the crack approaching the same location from the adjoining cell. For  $s/d < 3$ , and as shown in Fig. 4 for  $s/d = 1.5$ , the breakout cones of neighboring anchors intersected with each other as a result of the attraction of their fronts to the zero-shear stress vertical boundaries; these boundaries acted in a similar fashion to free surfaces that are known to attract cracks. The points of instability for this relatively small anchor spacing occurred at crack lengths roughly half of the length that they traveled before breaking the vertical boundary. When the crack fronts of neighboring unit cells approached each other, the assumption of axial symmetry became increasingly unrealistic. But because the ultimate load was achieved long before this happened, the results of the simulations were expected to be highly relevant.

The result that the maximum force during a pullout failure was achieved after a relatively small amount of crack growth underscores the fact that load carrying capacities dominated by fracture mechanics, unlike those involving net-section yielding, do not scale with the total area of the failure surface.

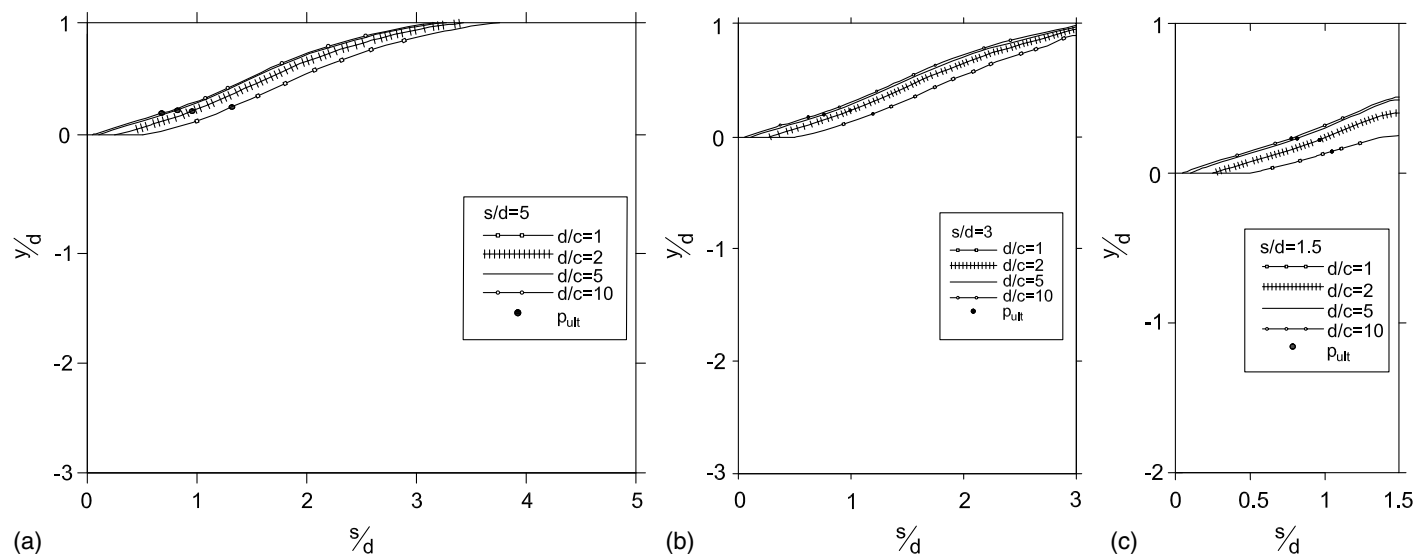


**Fig. 4.** Anchor paths for (a)  $s/d = 5$ ; (b)  $s/d = 3$ ; and (c)  $s/d = 1.5$ , indicating point of instability under load control

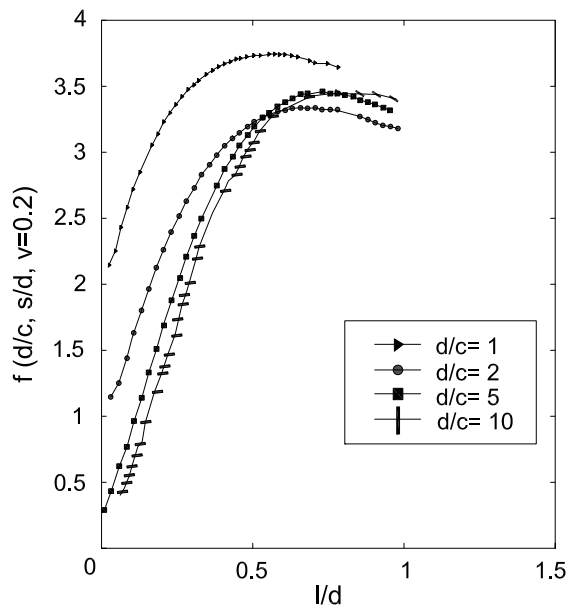


**Fig. 5.** Representative normalized Mode-I stress intensity factor as functions of normalized crack length ( $s/d = 3$ ,  $d/c = 1, 2, 5$ , and  $10$ )

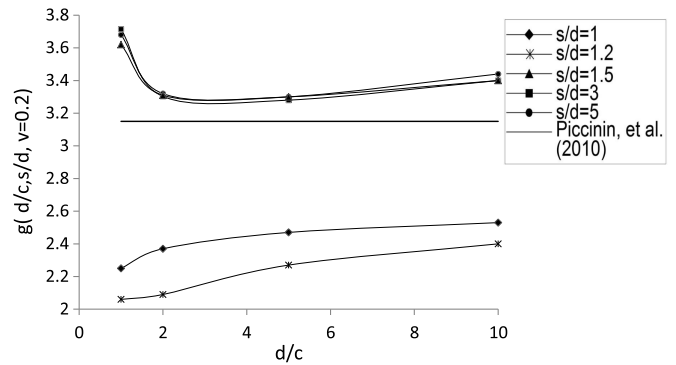
### Load-Carrying Capacity

Fig. 5, corresponding to  $s/d = 3$ , was representative of the previously defined normalized Mode-I stress intensity factor,  $f$ , as functions of crack length. For each normalized embedment depth, the curves on this plot produced the normalized maximum applied force,  $g$ , as defined by Eq. (4). The load-carrying capacity was shown as functions of embedment depth for selected values of anchor spacing that corresponded to the transition from no interaction to strong interaction between neighboring anchors.

Fig. 6 shows that the normalized capacities were weak functions of relative embedment depth,  $d/c$  (approximately 10%). As mentioned previously, the results for the largest three spacings were slightly different than those presented in Vogel and Ballarini (1999) and Piccinin et al. (2010, 2012). Specifically, for  $d/c > 2$ , the results showed the capacity to be a weak function of  $d/c$  that varied from approximately 3.2 to 3.4. Piccinin et al. (2010) reported instead an asymptote equal to 3.15; this study reproduced their results by using the displacement correlation technique, but the results presented in Fig. 6 are more accurate. Thus the  $d^{3/2}$  term sufficed to quantify the dependence of capacity on embedment depth. However, the load-carrying capacity was a moderately strong function of relative spacing,  $s/d$ , decreasing from an average value of approximately 3.3 for noninteracting anchors to approximately 2.3 for the smallest of the simulated spacings. The number of illustrative examples presented previously was not sufficient to derive a sufficiently accurate fit of the surface that represented the load-carrying capacity dependence on the embedment depth and anchor spacing. For the purposes of this paper, the plots of these dependencies, included in Fig. 6, should suffice. As discussed next, the reduction with decreased spacing was much less than what was dictated by available design formulas.

### Comparison with Currently Available Design Procedures

ACI-318-08 (ACI 2008) (Appendix D, Formula D-4), provides formulas that could be used to determine the nominal concrete



**Fig. 6.** Normalized load capacity as functions of normalized embedment depth ( $s/d = 1, 1.2, 1.5, 3$ , and  $5$ )

breakout tensile strength of a group of anchors with effective embedment depth,  $h_{ef}$ , with spacing,  $s < 3h_{ef}$ . This strength, normalized by the load-carrying capacity of a single anchor, is proportional to the ratio of the projected concrete failure area produced by the  $N$ -anchor group,  $A_{Nc}$ , to the reference area associated with a single anchor,  $A_{Nco} = 9h_{ef}^2$ . For the case of a square array of anchors the projected area is given by

$$A_{Nc} = \left[ (\sqrt{N} - 1)s + 3d \right]^2 \quad (5)$$

The force carried by one anchor in the group,  $P_{ult,N}/N$ , relative to the capacity of a single anchor,  $P_{ult,o}$ , therefore can be written as

$$\frac{P_{ult,N}}{NP_{ult,o}} = \frac{[(\sqrt{N} - 1)\frac{s}{3d} + 1]^2}{N} \quad (6)$$

A comparison between the periodic group studied in this paper and the code's design formulas can be made with  $h_{ef} \sim d$  and by setting  $N = \infty$ , which leads to

$$\frac{P_{ult,N=\infty}}{NP_{ult,o}} = \left( \frac{s}{3d} \right)^2 \quad (7)$$

For the values of relative spacing simulated in this paper,  $s/d = 5, 3, 1.5, 1.2$ , and  $1.0$ , the capacity ratios according to Eq. (7) are 1.0, 1.0, 0.25, 0.16, and 0.11, respectively (for  $s/d = 5$  and  $s/d = 1$ , the code considers the anchors as noninteracting). The 75–90% range of the reduction prescribed by the code was significantly larger than the ~20–30% reduction predicted by the simulations (Fig. 6).

The design codes are conservative; it was a necessary condition for minimizing potential structural failures. But this conservatism was partly because of the fact that the design formulas maintain that the load-carrying capacity is proportional to the projected areas associated with the failure cones.

### Conclusions

The results of the discrete crack propagation simulations presented in this paper, despite being limited to a simplified configuration involving a periodic arrangement of anchors, underscore the fact that the failure cones produced as steel anchors break out from a concrete matrix and are byproducts of the crack propagation, and that they are not related directly to the load-carrying capacity of the anchor group. This suggests that if less conservative designs are desired, one may start by abandoning the introduction of the

projected area of the failure cone into predictive equations, and instead, develop design formulas for specific anchorage configurations and applied loading from the results of three-dimensional LEM simulations of the breakout process in specific geometries subjected to specific loadings. Such efforts are realistic considering the advent of highly efficient and accurate finite element methods for three-dimensional crack propagation simulations.

## References

- ACI (American Concrete Institute). (1989). "Code requirements for nuclear safety." *ACI #349.1R*, Detroit.
- ACI (American Concrete Institute). (2006). "Code requirements for nuclear safety related concrete structures (ACI 349-06) and commentary (349R-06)." *ACI 349-06, 349R-06*, Detroit.
- ACI (American Concrete Institute). (2008). "Building code requirements for structural concrete (ACI 318-08) and commentary (318R-08)." *ACI 318-08, 318R-08*, Detroit.
- Ballarini, R., Keer, L. M., and Shah, S. P. (1987). "An analytical model for the pull-out of rigid anchors." *Int. J. Fract.*, 33(2), 75–94.
- Ballarini, R., Shah, S. P., and Keer, L. M. (1986). "Failure characteristics of short anchor bolts embedded in a brittle material." *Proc. R. Soc. London, A404*, 35–54.
- Elfgren, L. (1998). "Round robin analyses and tests of anchor bolts in concrete structures." *RILEM technical committee 90-FMA: Fracture mechanics of concrete applications*, RILEM, Cachan Cedex, France.
- Elfgren, L., and Ohlsson, U. (1992). "Anchor bolts modeled with fracture mechanics." *Application of fracture mechanics to reinforced concrete*, A. Carpinteri, ed., Elsevier, London.
- Eligehausen, R., and Balogh, T. (1995). "Behavior of fasteners loaded in tension in cracked reinforced concrete." *ACI J.*, 92(3), 365–379.
- Eligehausen, R., Malleé, R., and Silva, J. (2006). *Anchorage in concrete construction*, Ernst and Sohn, Berlin.
- Eligehausen, R., and Sawade, G. (1989). "Analysis of anchorage behaviour (literature review)." *Fracture mechanics of concrete structures: From theory to applications*, L. Elfgren, ed., Chapman and Hall, London.
- FRANC-2D [Computer software]. Cornell Fracture Group, Ithaca, NY.
- Fuchs, W., Eligehausen, R., and Breen, J. E. (1995). "Concrete capacity design (CCD) approach for fastening to concrete." *ACI J.*, 92(1), 73–94.
- Gordeliy, E., Piccinin, R., Napier, J. A. L., and Detournay, E. (2013). "Axisymmetric benchmark solutions in fracture mechanics." *Eng. Fract. Mech.*, 102, 348–357.
- Karihaloo, B. L. (1996). "Pull-out of axisymmetric headed anchors." *Mater. Struct.*, 29(3), 152–157.
- Klinger, R. E., and Mendonca, J. A. (1982). "Tensile capacity of short anchor bolts and welded studs: A literature review." *ACI J.*, 79(27), 270–279.
- Krenchel, H., and Shah, S. P. (1985). "Fracture analysis of the pullout test." *Mater. Struct.*, 18(6), 439–446.
- Ozbolt, J., and Eligehausen, R. (1992). "Fastening elements in concrete structures—Numerical simulations." *Proc., Fracture of Concrete and Rock, 2nd Int. Conf.*, H. P. Rossmanith, ed., E & FN Spon, London.
- Ozbolt, J., Eligehausen, R., and Reinhardt, H. W. (1999). "Size effect on the concrete cone pull-out load." *Int. J. Fract.*, 95(1–4), 391–404.
- Piccinin, R., Ballarini, R., and Cattaneo, S. (2010). "Linear elastic fracture mechanics pullout analyses of headed anchors in stressed concrete." *J. Eng. Mech.*, 10.1061/(ASCE)EM.1943-7889.0000120, 761–768.
- Piccinin, R., Ballarini, R., and Cattaneo, S. (2012). "Pullout capacity of headed anchors in prestressed concrete." *J. Eng. Mech.*, 10.1061/(ASCE)EM.1943-7889.0000395, 877–887.
- Vogel, A., and Ballarini, R. (1999). "Ultimate load capacities of plane and axisymmetric headed anchors." *J. Eng. Mech.*, 10.1061/(ASCE)0733-9399(1999)125:11(1276), 1276–1279.